arXiv:1512.07587v7 [cs.LG] 8 Jun 2016

A Latent-Variable Lattice Model

Rajasekaran Masatran MASATRAN@FREESHELL·ORG
Computer Science and Engineering, Indian Institute of Technology Madras

Abstract

Markov random field (MRF) learning is intractable, and its approximation algorithms are computationally expensive. We target a small subset of MRF that is used frequently in computer vision. We characterize this subset with three concepts: Lattice, Homogeneity, and Inertia; and design a non-markov model as an alternative. Our goal is robust learning from small datasets. Our learning algorithm uses vector quantization and, at time complexity $O(U \log U)$ for a dataset of U pixels, is much faster than that of general-purpose MRF.

1. Introduction

In computer vision, the MRF is commonly used to model images and videos. MRF algorithms are intractable in the general case, and approximation algorithms are generally used. The approximation algorithms themselves are computationally expensive. For computer vision, we usually do not need the full expressive power of MRF. In this paper, we restrict ourselves to a small subset of MRF that is useful for computer vision, and develop fast algorithms that work for this restricted case. We have three restrictions:

Lattice An image is a two-dimensional lattice.

Homogeneity The potentials and conditional probabilities are homogeneous across the lattice.

Inertia Nearby nodes are likely to be in the same state.

1.1. Markov Random Field

$G = (V, E)$ denotes an undirected graph. V is the set of nodes and E is the set of undirected edges. X_i denotes the variable associated with node i, for $i \in V$; giving a random vector $X = \{X_1, \cdots, X_p\}$. The local markov property for variable X_i states that X_i given its set of neighbors $X_{N(i)}$ is conditionally independent of the rest of the variables. A markov random field over a graph G is the set of distributions which satisfies all markov properties of G. $P(X) = \frac{1}{Z} \prod_{C \in \mathbb{C}} \phi_C(X_C)$ where C is a clique, and $\mathbb{C}$ is the set of cliques. $\phi_C(X_C)$ is the potential function of clique C, and Z is the normalization factor.

1.2. Lattice

We restrict our domain to d-dimensional lattices. Without loss of generality, we assume that the lattice has the same length, T nodes, in each dimension. Each node t is an element of $\{1 \cdots T\}^d$. We denote the lattice by T^d. These T^d nodes are latent variables and are hidden. Each of these has an associated visible variable that is not counted among its neighbors. The value of each visible variable is dependent solely on its latent variable. Given the values of all latent variables, the visible variables are independent of each other. q_t is the state of node t.

$S = \{S_1, S_2, \cdots S_j, \cdots S_N\}$ is the set of states.

$Q = \{q_t\}$ is the state of all latent variables.

$O = \{o_1, o_2, \cdots o_T\}$ is the set of observation symbols.

$R(t)$ is the set of $2\,d$ nodes adjacent to node t.

$U = \sum T^d$ is the set of all pixels.

1.3. Homogeneity

Due to the markov property, $P(q_t|Q \setminus q_t) = P(q_t|Q(R(t)))$. We consider only the case where $\phi(t, r \in R(t))$, as well as $P(o_t = v_k|q_t = S_j)$ are independent of t. Therefore, we represent $\phi(t, r \in R(t))$ by a common matrix A, and $P(o_t = v_k|q_t = S_j)$ by a common matrix B.

$N = |S|$; $S = \{S_1, S_2, \cdots S_j, \cdots S_N\}$ are the unique states in the model, and the state at node t is q_t.

$M = |V|$; $V = \{v_1, v_2, \cdots v_k, \cdots v_M\}$ are the unique observation symbols, and the symbol at node t is o_t.

$A = \{a(i,j)\}$; $a(i,j) = \phi(q_t = S_j, q_{r \in R(t)} = S_i)$, the state adjacency potential function.

$B = \{b(j,k)\}$; $b(j,k) = P(o_t = v_k|q_t = S_j)$, the observation symbol probability distribution in state j.

1.4. Associativity

In a latent-variable model, if adjacent latent nodes share the same set of possible states, and are likely to be in the same state, this is called associativity. This is an intrinsic property of the process underlying many application domains. The amount of associativity in the lattice varies by domain. In the one-dimensional case, there is a lot of associativity in speech recognition, a limited amount of associativity in chunking of natural language, and almost no associativity in part-of-speech tagging in natural language.

We propose an index for associativity: $\boxed{\sum_i a_{i,i} / \sum_{i,j} a_{i,j}}$. It is 0 when adjacent nodes are uncorrelated, and 1 when adjacent nodes are always in the same state. Our model should be applicable when this index is atleast, say, 0.5.

1.5. Inertia

Associativity is restricted to dependency between adjacent latent nodes. In this paper, we consider a broader condition, where non-adjacent latent nodes are dependent on each other. This is not markov, but is related to an n^{th}-order markov model. We call this inertia, and restrict our model to lattices with inertia. Since an inertial model can approximate an associative model, it can be used for: (1) Applications with inertia in the lattice, as well as (2) Approximation of applications with associativity in the lattice.

We use a sliding hypercube window to propose an index for inertia: $\boxed{\mathbb{E}\left[\sqrt{\sum_j {p_j}^2}\right]}$. The expectation is taken over the hypercube centered at the node, for every node in the lattice. p_j is the probability of state S_j in the window. It is 1 when all nodes in the window are in the same state, and $\frac{1}{\sqrt{N}}$ when all states have equal probability within the window. Our model should be applicable when this index is atleast, say, 0.9.

1.6. Examples

In the following figures, each circle is a MRF node. The thick circles are latent-variable nodes. Figure 1 is an associative MRF, while Figure 2 is a non-associative MRF. The matrices are pairwise potentials, and the main diagonal represents adjacent nodes being in the same state. All nodes, latent and visible, are boolean. Differences between the two MRFs are highlighted in bold.

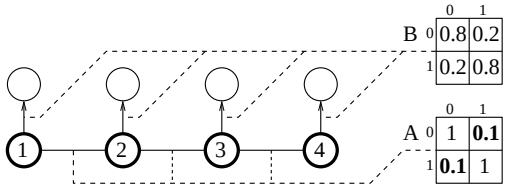


Figure 1. Associative MRF

Figure 1 is an associative MRF. It has parameters: S: $\{0,1\}$, V: $\{0,1\}$, A: $\left(\begin{smallmatrix} 1 & \mathbf{0.1} \\ \mathbf{0.1} & 1 \end{smallmatrix}\right)$, B: $\left(\begin{smallmatrix} 0.8 & 0.2 \\ 0.2 & 0.8 \end{smallmatrix}\right)$. The index of associativity is: $\frac{1+1}{1+0.1+0.1+1} = 0.91$.

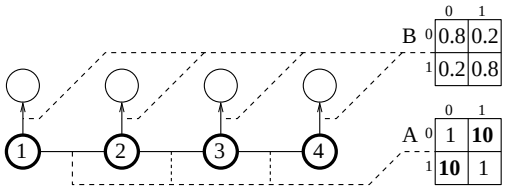


Figure 2. Non-Associative MRF

Figure 2 is an non-associative MRF. It has parameters: S: $\{0,1\}$, V: $\{0,1\}$, A: $\left(\begin{smallmatrix} 1 & \mathbf{10} \\ \mathbf{10} & 1 \end{smallmatrix}\right)$, B: $\left(\begin{smallmatrix} 0.8 & 0.2 \\ 0.2 & 0.8 \end{smallmatrix}\right)$. The index of associativity is: $\frac{1+1}{1+10+10+1} = 0.09$.

1.7. Using Stochastic Models

An assignment of observed symbol to each visible variable is an image. The image is essentially the visible-variable lattice, as opposed to the latent-variable lattice. Our training data consists of images, and lacks the state configuration of the corresponding latent variables.

In classification of images, the input is a set of classes that are specified by a set of images belonging to each. The objective is to classify test images into these classes. We build a model for each class by learning a class-conditional density for its lattice configurations. Given the prior probabilities and these class-conditional models, bayesian classification is used to classify test images.

1.8. Prior Work

Graphical models for general networks were introduced in (Pearl, 1988). (Blake et al., 2011) discussed MRF applications in computer vision. *In Physics*, the Ising model is widely used. The Potts model, described in (Wu, 1982), is a generalization of the Ising model, and is closely related to MRF. *Our main benchmark* is the algorithm for fast inference in associative pairwise MRF in (Boykov et al., 2001). We solve a slightly different problem, and our solution should be useful in approximating a solution to associative MRF as well.

1.9. Contributions

1. *A latent-variable statistical model for lattice-structured data*: a variant each, for the discrete case (Section 2) and the real case (Section 3)

2. An index for associativity (Subsection 1.4)

3. An index for inertia (Subsection 1.5)

2. Our Model

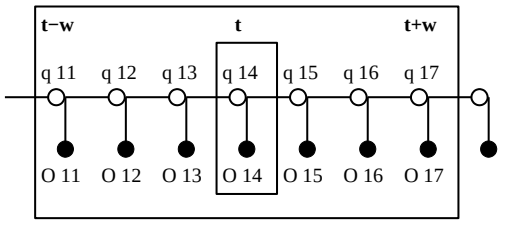
In this section, we describe the variant of our model for discrete output symbols. The one-dimensional case of this variant can be used to model, for instance, proteins, which are sequences of twenty amino acids.

The signature, discussed in section 3.3, maps the node into the probability simplex. We divide the probability simplex into partitions, and a partition corresponds to a state in MRF. The potential between partitions is A, and the observation symbol probability distribution is B. Roughly, this is our data model. Our model is not markov. It has inertia. The parameter set of our model is $\eta = \langle A, B, w \rangle$.

2.1. Probability Simplex

The range of the probability mass for a multinomial distribution with M categories is the is the standard $(M-1)$ simplex, $\left\{(p_1, p_2, \cdots p_n) \in \mathbb{R}^M \mid \sum_{k=1}^{n} p_k = 1, p_k \geq 0\right\}$. The states of a MRF can be considered points in the probability simplex. The coordinates of the state are the observation symbol probability distribution B.

2.2. Sliding Window



Sliding window methods are popular for sequences (Dietterich, 2002) and images. Since our model has inertia, nearby nodes are probably in the same state. Therefore, sliding window models are likely to work well. At t, the w-window is the hypercube from $(t - [w, w, \cdots])$ to $(t + [w, w, \cdots])$. It might be beneficial to use different values of w for evaluation, decoding and learning: w_e for evaluation, w for decoding, and w_l for learning.

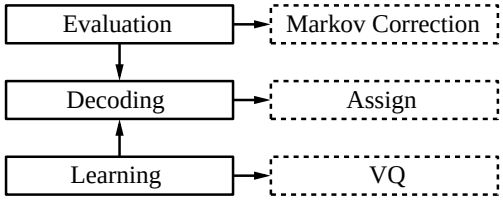
2.3. Bias-Variance Tradeoff

The optimal size of the window is related to the typical minimum number of steps in the same direction before a change of state. Increasing the window size increases inductive bias, and reduces variance. Reducing the window size reduces inductive bias, and increases variance.

2.4. Signature

Our decoding algorithm works in two steps: (1) Characterize the sliding window around the current node with a signature, and (2) Use this signature to assign a latent state to the current node. The signature X is that observation probability vector with maximum likelihood of generating the symbols in the sliding window. $X = \{x_t(k)\}$ where $x_t(k)$ is the sample probability of symbol v_k in the w-window around node t. This signature is a point in the probability simplex.

2.5. Algorithms and their Dependencies



2.6. Evaluation

Given the model $\eta = \langle A, B, w \rangle$ and the image O, compute the probability $P(O|\eta)$ that the image was produced by the model.

Algorithm 1: Evaluation ($O(MNT^d)$)

Input: A, B, w_e, O
Output: p
$(X, Q) \leftarrow decoding(B, w_e, O)$ $\quad$ $\underline{O(MNT^d)}$
$p \leftarrow 1$
for $t \in T^d$ **do**
  $k \leftarrow \sum_{r \in R(t)} a(q_t, q_r)$
  $p \leftarrow p\, b(q_t, o_t) \sqrt{\prod_{r \in R(t)} \alpha(X, t)^{\frac{a(q_t, q_r)}{k}}}$
  Represent in log domain to prevent underflow.
end

Algorithm 1: Since we have inertia, the results of the decoding algorithm are reliable, and we do not need to consider all possible lattice configurations. We decode the lattice configuration from the image, and use that to compute the likelihood.

2.7. Markov Correction

$0 < \alpha(X, t) \leq 1$ corrects for assuming the markov property in the evaluation step though it is not present in this model. Experimental evaluation is required to determine typical values.

2.8. Decoding

Find the lattice configuration $Q = \{q_t\}_{t \in T}$, given the model $\eta = \langle A, B, w \rangle$ and the image O.

Algorithm 2: To decode the lattice, we initialize the sliding window and compute the symbol counts (*symcount*) in it. We slide the sliding window through the lattice, and in every step, update the symbol counts, and send the signature

Algorithm 2: Decoding ($O(MNT^d)$)

Input: B, w, O
Output: X, Q
Initialize$_{v_k \in V}$ $symcount(v_k)$
for $t \in T^d$ **do** $\underline{O(MNT^d)}$
  $x_t \leftarrow \frac{symcount}{M}$
  $q_t \leftarrow assign(B, x_t)$ $\underline{O(MN)}$
  increment $symcount(newwindow - oldwindow)$
  decrement $symcount(oldwindow - newwindow)$
end

of the sliding window to *assign* to get the node state.

2.9. Assign

The assign subroutine finds the node state $q_t \in S$, given the model $\eta = \langle A, B, w \rangle$ and the node signature x_t.

Algorithm 3: Assign ($O(MN)$)

Input: B, x_t
Output: q_t
for $j \leftarrow 1$ **to** N **do** $\underline{O(MN)}$
  $dist(j) \leftarrow \|x - B(j)\|$
end
$q_t \leftarrow \min \text{index}_j(dist_j)$

Algorithm 3: Since the model has inertia, we reduce computational complexity of assigning state by assuming that neighboring nodes probably have the same state as the current node.

The node signature x_t is a probability distribution. The $assign$ subroutine assigns t to that state j for which $B(j)$ is the closest to x_t, as per L_2 norm. This creates a partitioning of the probability simplex into partitions, each of which is associated with a state.

2.10. Learning

Optimize the model parameters $\eta = \langle A, B, w \rangle$ to best describe the image, i.e., maximize $P(O|\eta)$.

Algorithm 4: Since we have inertia, our decoding algorithm is reasonably reliable. We decode the image, and use the lattice configuration to learn the parameters of the model.

We compute the signature at all nodes using symbol counts (*symcount*). Vector quantization on the signatures partitions the probability simplex into states. The coordinates of the centroids are the observation probability matrix, and the sample transition probabilities in the lattice of signatures are the state potential matrix.

Algorithm 4: Learning ($O(MU \log U)$)

Input: O, w_l
Output: A, B
Initialize$_{v_k \in V}$ $symcount(v_k)$
for $t \in U$) **do** $\underline{O(MU)}$
  $x_t \leftarrow \frac{symcount}{M}$ $\underline{O(M)}$
  increment $symcount(newwindow - oldwindow)$
  decrement $symcount(oldwindow - newwindow)$
end
$(B, Q) \leftarrow VQ(X)$ $\underline{O(MU \log U)}$
$\underline{B \text{ is assigned the VQ codebook.}}$
for $t \in U$ **do** $\underline{O(U)}$
  increment $statecount(q_t)$
  for $r \in R(t)$ **do**
    increment $A'(q_t, r)$
  end
end
for $j \leftarrow 1$ **to** N **do**
  $A(j) \leftarrow \frac{A'(j)}{2\ d\ statecount(j)}$
end

2.11. Vector Quantization

Our requirements for clustering are: (1) Roughly spherical partitions, and (2) A representative point for each partition. We solve our clustering problem as vector quantization (VQ) since the requirements are similar. VQ is a classical technique from signal processing that models probability density functions by the distribution of prototype vectors. There are multiple VQ algorithms with different tradeoffs. Fast pairwise nearest neighbor (Fast PNN) from (Equitz, 1989) is a VQ algorithm that trades modeling accuracy for reduced computational complexity. We use Fast PNN as it has $O(n \log n)$ computational complexity, and we do not need high modeling accuracy in VQ.

2.12. Time Complexity

	Our Model
Evaluation	$O(MNT^d)$
Decoding	$O(MNT^d)$
Learning	$O(MU \log U)$

3. Extension to Real Symbols

In this section, we describe the variant of our model for real-valued, as opposed to discrete, output symbols. The two-dimensional case of this variant can model digital images, in grayscale pixel value, or in extracted features. Previously, the state variable took values in the probability simplex embedded in $\mathbb{R}^M$. Now, it consists of M real variables representing the mean vector, i.e., it is a M-dimen-

sional vector and has range $\mathbb{R}^M$. $o_t = \{o_{t,1}, o_{t,2}, \cdots o_{t,M}\}$. The parameter set of this variant is $\eta = \langle A, \mu, \Sigma, w \rangle$.

When each point is assigned to the closest state, the state space gets divided into partitions, each of which corresponds to a state in MRF. Matrix A remains the probability of transitioning between partitions, and w remains the size of the sliding window. We modify the other parameters of our model as follows:

$M = |V|$ was the number of unique observation symbols. Instead, now the observation symbol o_t is in $\mathbb{R}^M$.

B was the observation symbol probability distribution. It is replaced by μ and Σ.

$\mu = \mu(j, k)$; where $\mu(j)$ is the sample mean of state S_j.

$\Sigma = \Sigma(j, i, k)$; where $\Sigma(j)$ is the sample covariance matrix of state S_j.

3.1. Prior Work

Real-symbol HMM is discussed in subsection IV-A of (Rabiner, 1989). Switching linear dynamical systems (LDS) are an extension of HMM in which each state is associated with a linear dynamical process. (Fox et al., 2011) describes inference in switching LDS and switching vector autoregressive (VAR) processes.

3.2. Signature

The signature is the estimated mean of the distribution that generated the symbols in the sliding window. In the w-window around node t, the signature is the sample mean x_t of the symbols in the sliding window.

3.3. Evaluation

Given the model $\eta = \langle A, \mu, \Sigma, w \rangle$ and the image O, compute the probability $P(O|\eta)$ that the image was produced by the model.

Algorithm 5: Evaluation ($O(MNT^d)$)

Input: A, μ, Σ, w_e, O
Output: p
$(X, Q) \leftarrow decoding(\mu, \Sigma, w_e, O)$ $\quad \underline{O(MNT^d)}$
$p \leftarrow 1$
for $t \in T^d$ **do** $\quad \underline{O(M^2T^d)}$
  $k \leftarrow \sum_{r \in R(t)} a(q_t, q_r)$
  $p \leftarrow p\ f(o_t|\mu(q_t), \Sigma(q_t))\ \sqrt{\prod_{r \in R(t)} \alpha(X, t)^{\ \frac{a(q_t, q_r)}{k}}}$
  $\underline{f(o|\mu, \Sigma)}$: Normal distribution.
  Represent in log domain to prevent underflow.
end

Algorithm 5: Since the clusters generated by VQ all have the same size, there is no prior probability term in the probability update.

3.4. Decoding

Find the lattice configuration $Q = \{q_1, q_2, \cdots q_T\}$, given the model $\eta = \langle A, \mu, \Sigma, w \rangle$ and the image O.

Algorithm 6: Decoding ($O(MNT^d)$)

Input: μ, Σ, w, O
Output: X, Q
Initialize sum
for $t \in T^d$ **do** $\quad \underline{O(MNT^d)}$
  $x_t \leftarrow \frac{sum}{M}$
  $q_t \leftarrow assign(\mu, \Sigma, x_t)$ $\quad \underline{O(MN)}$
  increment $sum(newwindow - oldwindow)$
  decrement $sum(oldwindow - newwindow)$
end

Algorithm 6: We initialize the sliding window and compute the sum of the output instances in it. We slide the sliding window to the end, and in every step, we update the sum and send the signature of the sliding window to *assign* to get the state lattice.

3.5. Assign

The assign subroutine finds the state $q_t \in S$, given the model $\eta = \langle A, \mu, \Sigma, w \rangle$, and a node signature x_t.

Algorithm 7: Assign ($O(MN)$)

Input: μ, x_t
Output: q_t
for $j \leftarrow 1$ **to** N **do** $\quad \underline{O(MN)}$
  $dist(j) \leftarrow \|x_t - \mu(j)\|$
end
$q_t \leftarrow \min \text{index}_j(dist_j)$

Algorithm 7: The $assign$ subroutine assigns t to that state j for which $\mu(j)$ is the closest to x_t.

3.6. Learning

Optimize the model parameters $\eta = \langle A, \mu, \Sigma, w \rangle$ to best describe how an image comes about, i.e., maximize $P(O|\eta)$. (See Algorithm 8)

3.7. Time Complexity

The time complexities are the same as the original model. In case N and M are not considered constant, these caveats apply: (1) In Algorithm 5, $O(M^2T^d)$ is assumed to be less

Algorithm 8: Learning ($O(MU \log U)$)

Input: O, w_l
Output: A, μ, Σ
Initialize sum
for $t \in U$ **do** $\underline{O(MU)}$
  $x_t \leftarrow \frac{sum}{M}$ $\underline{O(M)}$
  increment $sum(newwindow - oldwindow)$
  decrement $sum(oldwindow - newwindow)$
end
$(\mu, Q) \leftarrow VQ(X)$ $\underline{O(MU \log U)}$
  $\underline{\mu \text{ is assigned the VQ codebook.}}$
for $t \in U$ **do** $\underline{O(M^2U)}$
  increment $statecount(q_t)$
  for $r \in R(t)$ **do**
    increment $A'(q_t, r)$
  end
  $y \leftarrow (o_t - \mu(q_t))$
  $\Sigma'(q_t) \leftarrow \Sigma'(q_t) + yy'$ $\underline{O(M^2)}$
end
for $j \leftarrow 1$ **to** N **do**
  $A(j) \leftarrow \frac{A'(j)}{2\ d\ statecount(j)}$
  $\Sigma(j) \leftarrow \frac{\Sigma'(j)}{statecount(j)}$
end

than $O(MNT^d)$, since $O(M)$ is usually less than $O(N)$, and (2) In Algorithm 8, $O(M^2U)$ is assumed to be less than $O(MU \log U)$, since $O(M)$ is usually less than $O(\log U)$.

4. Conclusion

We have designed an alternative model for a subclass of MRF that is used frequently in computer vision. We have two variants: one for lattices of discrete symbols, and one for lattices of vectors. Our learning algorithm, at time complexity $O(U \log U)$, is significantly faster than algorithms of general-purpose MRF. We are currently evaluating our model on the PASCAL VOC Challenge 2006 (Everingham et al., 2006).

4.1. Advantages

1. Variance component of error is low.
2. Uses small datasets efficiently.
3. Computational complexity is low.
4. Easily extends to a quadtree approach.

4.2. Disadvantages

1. Bias component of error is high.
2. Does not use large datasets efficiently.
3. Modeling accuracy is low.
4. N, w, and β need to be chosen appropriately.

4.3. Future Work

1. A quadtree approach can provide progressive results.
2. The model can be repeated multiple times, each with a different window size, and combined into a factorial model.
3. A theoretical framework can be developed for guarantees on modeling accuracy.
4. Estimating a belief-state instead of a vanilla state might give better accuracy.
5. N can be learned from the data.
6. w can be learned from the data.

Acknowledgments: Gowthaman Arumugam.

References

Blake, Andrew, Kohli, Pushmeet, and Rother, Carsten. *Markov Random Fields for Vision and Image Processing*. MIT Press, 2011. ISBN 0262015773, 9780262015776.

Boykov, Yuri, Veksler, Olga, and Zabih, Ramin. Fast Approximate Energy Minimization via Graph Cuts. *IEEE Transactions on Pattern Analysis and Machine Intelligence*, 23(11):1222–1239, 2001.

Dietterich, Thomas G. Machine Learning for Sequential Data: A Review. In *Structural, Syntactic, and Statistical Pattern Recognition*, volume 2396 of *LNCS*, pp. 15–30, 2002.

Equitz, William H. A New Vector Quantization Clustering Algorithm. *IEEE Transactions on Acoustics, Speech and Signal Processing*, 37(10):1568–1575, 1989.

Everingham, Mark, Zisserman, Andrew, Williams, Chris K. I., and van Gool, Luc. The PASCAL Visual Object Classes Challenge 2006 Results, 2006.

Fox, Emily B., Sudderth, Erik B., Jordan, Michael I., and Willsky, Alan S. Bayesian Nonparametric Inference of Switching Dynamic Linear Models. *IEEE Transactions on Signal Processing*, 59(4):1569–1585, 2011.

Pearl, Judea. *Probabilistic Reasoning in Intelligent Systems: Networks of Plausible Inference*. Morgan Kaufmann Publishers, 1988. ISBN 0-934613-73-7.

Rabiner, Lawrence R. A Tutorial on Hidden Markov Models and Selected Applications in Speech Recognition. *Proceedings of the IEEE*, 77(2):257–286, 1989.

Wu, Fa-Yueh. The Potts Model. *Reviews of Modern Physics*, 54(1):235–268, 1982.